

CP violation and BSM Higgs bosons

Venus Keus*

*Department of Physics and Helsinki Institute of Physics,
Gustaf Hallstromin katu 2, FIN-00014 University of Helsinki, Finland
E-mail: venus.keus@helsinki.fi*

We study extensions of the Standard Model (SM) in which copies of the SM scalar $SU(2)$ doublet are added to the Higgs sector. These scalar doublets either acquire a Vacuum Expectation Value (VEV) and hence are *active* or do not develop a VEV and are *inert*. We consider CP-violation (CPV) in both the active and inert sector. As an example of a model with CPV in the active sector, we present a Type-I 2-Higgs-Doublet Model (2HDM) with two active doublets and show Large Hadron Collider (LHC) signals of such a scenario. The amount of CPV in this case is very limited due to constraints coming from Electric Dipole Moment experiments. Moreover, 2HDMs with only active doublets do not provide a Dark Matter (DM) candidate. As a result, we turn to 3-Higgs-Doublet Models (3HDMs) where unbounded CPV and viable DM candidates could be introduced simultaneously in the inert sector. We investigate DM phenomenology of such models.

*Prospects for Charged Higgs Discovery at Colliders
3-6 October 2016
Uppsala, Sweden*

*Speaker.

1. Introduction

The great success of the Standard Model (SM) was achieved in 2012 with the discovery of the long-awaited Higgs boson [1, 2], the last missing particle of the SM at the large Hadron Collider (LHC), as this particle was predicted by the Electro-Weak Symmetry Breaking (EWSB) mechanism in 1964. Even though no significant deviation from the SM has been observed so far, it is well understood that the SM of particle physics is not the complete theory of Nature. Many astrophysical observations require a Dark Matter (DM) which is stable on cosmological time scales, cold, non-baryonic, neutral and weakly interacting. The SM does not provide any such candidate. The most well-studied such candidates are the Weakly Interacting Massive Particles (WIMPs) [3, 4, 5], with masses between a few GeV and a few TeV. Such a WIMP candidate must be cosmologically stable, usually due to the conservation of a discrete symmetry, and must freeze-out to result in the observed relic density [6]:

$$\Omega_{\text{DM}} h^2 = 0.1199 \pm 0.0027. \quad (1.1)$$

Similarly the Baryon asymmetry of the Universe (BAU) which requires the CP-symmetry to be broken, cannot be explained by the SM since the amount of CP-violation (CPV) in SM does not lead to enough matter-antimatter asymmetry to match observational data [7, 8].

The simplest Beyond Standard Model (BSM) scenarios which aim to conquer these shortcomings are scalar extensions. 2-Higgs-Doublet Models (2HDMs) with one scalar $SU(2)$ doublet added to the SM could partly provide an answer. A 2HDM with two *active* doublets could accommodate CPV. In section 2, we study a Type-I 2-Higgs-Doublet Model (2HDM) with CPV and present signatures of this model for future discovery at the LHC. Since both doublets are active, the amount of CPV introduced here is very limited due to bounds coming from Electric Dipole Moment (EDM) experiments. Moreover, 2HDMs with CPV fall short on providing a DM candidate.

The Inert Doublet Model (IDM) [9] with one *inert* and one *active* doublet in the scalar sector, provides a viable DM candidate, the lightest neutral particle from the inert doublet. The IDM has been studied extensively in the last few years (see, e.g., [10, 11, 12]) where a discrete Z_2 symmetry unbroken after EWSB protects the DM from decaying into SM fields. Since the IDM involves 1 Inert Doublet plus 1 active Higgs Doublet, we shall also refer to it henceforth as the I(1+1)HDM. The I(1+1)HDM, though very constrained, remains a viable model for a scalar DM candidate, being in agreement with current experimental constraints. However, by construction, the I(1+1)HDM can not contain CPV; due to the presence of an exact Z_2 symmetry, all parameters in the potential are real. To incorporate both DM and CPV, we need to go beyond two scalar doublets.

In section 3, we study a 3-Higgs-Doublet model (3HDM) with 2 inert Higgs plus 1 active Higgs doublet which provides a viable DM candidate and unbounded amount of CPV arising from the inert sector. We refer to this model as the I(2+1)HDM. Here, the active sector is identical to that of the SM and the inert sector is extended. CPV is introduced in the inert sector and the neutral inert particles now have a mixed CP quantum number.

2. CP-violating 2-Higgs-Doublet Models

2.1 The scalar potential

In the general form, the 2HDMs allow for Flavour Changing Neutral Currents (FCNCs) at

the tree level which have not been observed experimentally. To forbid these FCNCs, the scalar potential could be restricted by imposing a Z_2 symmetry which is also extended to the fermion sector. Depending on this Z_2 charge assignment on the fermions, four independent types of 2HDMs are defined [13, 14]. Here, we study the Type-I model where only one Higgs doublet, ϕ_1 , couples to fermions. The Z_2 charges of ϕ_1 and ϕ_2 is set to be even and odd, respectively.

The Z_2 symmetric 2HDM potential has the form:

$$V = \mu_1^2(\phi_1^\dagger \phi_1) + \mu_2^2(\phi_2^\dagger \phi_2) - \left[\mu_3^2(\phi_1^\dagger \phi_2) + h.c. \right] + \frac{1}{2}\lambda_1(\phi_1^\dagger \phi_1)^2 + \frac{1}{2}\lambda_2(\phi_2^\dagger \phi_2)^2 \\ + \lambda_3(\phi_1^\dagger \phi_1)(\phi_2^\dagger \phi_2) + \lambda_4(\phi_1^\dagger \phi_2)(\phi_2^\dagger \phi_1) + \left[\frac{1}{2}\lambda_5(\phi_1^\dagger \phi_2)^2 + h.c. \right]. \quad (2.1)$$

with the doublets compositions defined as

$$\phi_1 = \begin{pmatrix} \phi_1^+ \\ \frac{v_1 + h_1^0 + ia_1^0}{\sqrt{2}} \end{pmatrix}, \quad \phi_2 = \begin{pmatrix} \phi_2^+ \\ \frac{v_2 + h_2^0 + ia_2^0}{\sqrt{2}} \end{pmatrix}, \quad (2.2)$$

where v_1 and v_2 could be complex. We allow for the Z_2 soft-breaking term, μ_3^2 and take the Vacuum Expectation Values (VEVs) to be real and positive and defined as $v^2 \equiv v_1^2 + v_2^2 = (246 \text{ GeV})^2$ and the ratio of the two VEVs is $\tan\beta = v_2/v_1$. Therefore, CPV is introduced explicitly through the only complex terms in the potential, μ_3^2 and λ_5 . The minimisation conditions require

$$\text{Im}\mu_3^2 = \frac{v^2}{2} \text{Im}\lambda_5 s_\beta c_\beta. \quad (2.3)$$

Therefore $\text{Im}\lambda_5$ may be regarded as the only source of CPV. Throughout the paper, we will be using the following abbreviations: $s_\theta = \sin\theta$, $c_\theta = \cos\theta$ and $t_\theta = \tan\theta$.

We make use of the Higgs basis [15] where the rotated doublets are represented by $\hat{\phi}_i$

$$\begin{pmatrix} \hat{\phi}_1 \\ \hat{\phi}_2 \end{pmatrix} = \begin{pmatrix} c_\beta & s_\beta \\ -s_\beta & c_\beta \end{pmatrix} \begin{pmatrix} \phi_1 \\ \phi_2 \end{pmatrix}, \quad (2.4)$$

where $\langle \hat{\phi}_1 \rangle = v$ and $\langle \hat{\phi}_2 \rangle = 0$.

The mass of the charged Higgs boson, H^\pm , is calculated to be

$$m_{H^\pm}^2 = \frac{\text{Re}\mu_3^2}{s_\beta c_\beta} - \frac{v^2}{2}(\lambda_4 + \text{Re}\lambda_5). \quad (2.5)$$

The masses of the three neutral CP-mixed states, H_1 , H_2 and H_3 , is calculated by diagonalising the 3×3 mass-squared matrix where we assume $m_{H_1} \leq m_{H_2} \leq m_{H_3}$. The explicit form of the rotation matrix and Feynman rules are presented in [16]. In the following, we identify H_1 as the SM-like Higgs boson, so that we take $m_{H_1} = 125 \text{ GeV}$.

2.2 Constraints on the model

We have taken into account the stability of the Higgs potential, S-matrix unitarity and the S , T and U parameters [17, 18]. We also take into account EDMs which limit the CPV parameter, i.e., $\text{Im}\lambda_5$ significantly. The B physics data also provides constraints on the parameter space in

2HDMs, which are especially sensitive to m_{H^\pm} and $\tan\beta$. In addition, we also take into account the constraint from direct searches for extra Higgs bosons at the LHC.

Fig. 1 summarizes the bounds taken into account where we show the allowed parameter regions on the $\text{Im}\lambda_5$ and $\tan\beta$ plane. In this plot, we take $m_{H_2} = 200$ GeV, $m_{H_3} = m_{H^\pm} = 250$ GeV and $s_{\beta-\tilde{\alpha}} = 1$ where $\beta - \tilde{\alpha}$ is the mixing angle which diagonalises the CP-even Higgs states in the Higgs basis.

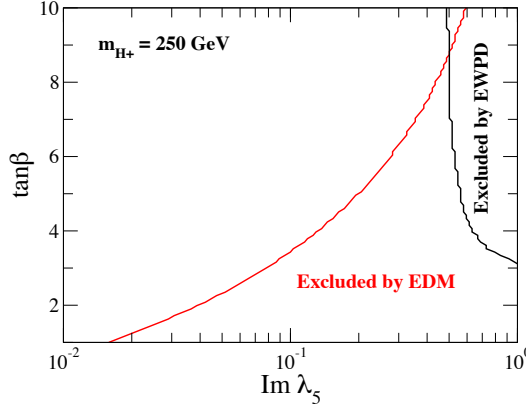


Figure 1: The constrained region in the $\text{Im}\lambda_5$ - $\tan\beta$ plane is shown in the case of $m_{H_2} = 200$ GeV, $m_{H_3} = m_{H^\pm} = 250$ GeV and $s_{\beta-\tilde{\alpha}} = 1$.

2.3 Phenomenology at the LHC

For our numerical results, we use the fixed input parameters $m_{H_2} = 200$ GeV and $m_{H_3} = m_{H^\pm} = 250$ GeV. In the top left plot in Fig. 2, we show the gauge-gauge-scalar couplings which are described by $g_{hVV}^{\text{SM}} \times \xi_V^{H_i}$ ($i = 1, 2, 3$) as a function of $\text{Im}\lambda_5$ where $\tan\beta = 10$ and $s_{\beta-\tilde{\alpha}} = 1$. The vertical dotted line shows the upper limit on $\text{Im}\lambda_5$. It is evident that, over the allowed values of $\text{Im}\lambda_5$, deviations of the SM-like Higgs couplings to W^+W^- and ZZ induced by CPV are negligible, thereby generating no tension against LHC data. We establish the W^+W^- and ZZ decays of all three Higgs states of the 2HDM Type-I as a hallmark signature of CPV.

On the top right plot in Fig. 2, we present the ratio of decay rates of the H_1 (identified as the SM-like Higgs boson) to those of h_{SM} (the Higgs boson in the SM) for $\tan\beta = 5$ and $s_{\beta-\tilde{\alpha}} = 0.98$. Over the allowed $\text{Im}\lambda_5$ region, none of BRs of the SM-like Higgs boson deviates significantly from the LHC data, except for $b\bar{b}$, $\tau^+\tau^-$ and gg . Therefore, this effect may be significant in order to establish CPV. Note that this occurs in a complementary region of the parameter space in comparison to where the W^+W^- and ZZ signals of the neutral Higgs states can be seen.

The bottom plot in Fig. 2 shows the signal strength, $\mu_{\chi\gamma}$, of the SM-like Higgs boson H_1 . CPV affects the signal strengths via the production cross sections, partial decay widths and the total decay width. Here, only the $\tau^+\tau^-$ channel may carry some evidence of CPV for $s_{\beta-\tilde{\alpha}} = 0.98$ and $\tan\beta = 5$. Hence, this offers a second channel to access CPV in the 2HDM Type-I studied here, alternative to the smoking gun signature of W^+W^- and ZZ decays.

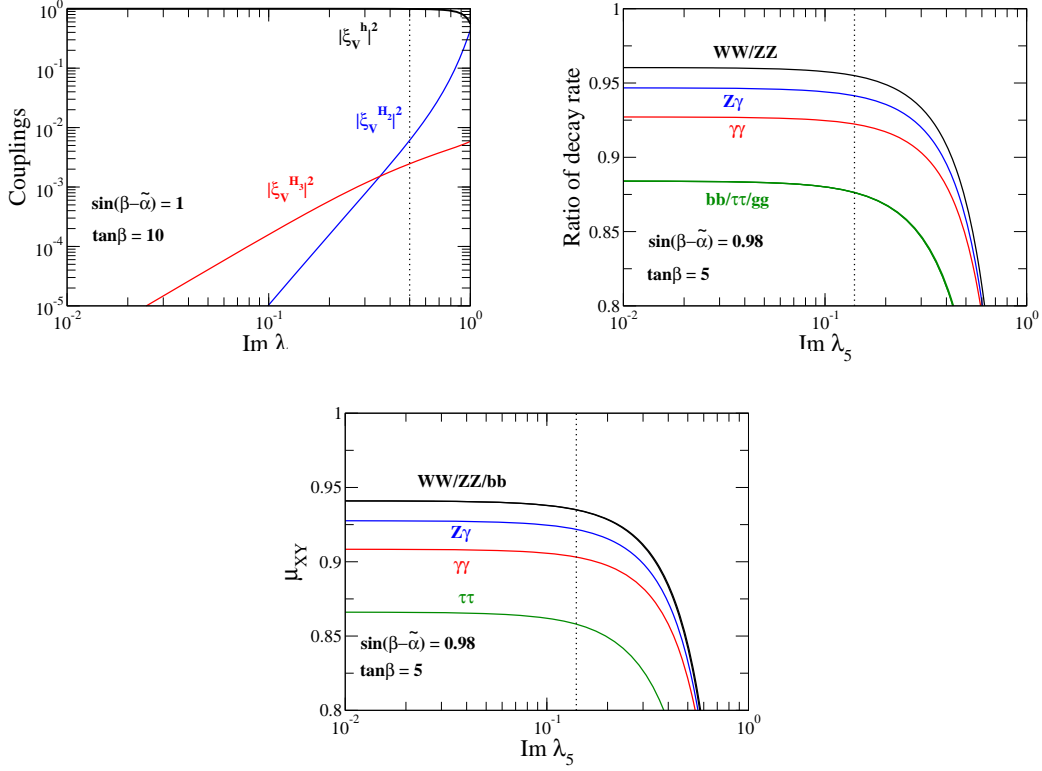


Figure 2: Signature of CPV in different regions of the parameter space.

3. CP-violating 3-Higgs-Doublet Models

3.1 The scalar potential

In this section we study a 3HDMs with 2 inert Higgs plus 1 active Higgs doublet which we refer to as the I(2+1)HDM. It has been shown [19] that a Z_2 -symmetric 3HDM potential¹, under whose symmetry the three Higgs doublets $\phi_{1,2,3}$ transform, respectively, as $g_{Z_2} = \text{diag}(-1, -1, 1)$, is of the following form:

$$\begin{aligned}
 V_{3HDM} = & -\mu_1^2(\phi_1^\dagger\phi_1) - \mu_2^2(\phi_2^\dagger\phi_2) - \mu_3^2(\phi_3^\dagger\phi_3) + \lambda_{11}(\phi_1^\dagger\phi_1)^2 + \lambda_{22}(\phi_2^\dagger\phi_2)^2 + \lambda_{33}(\phi_3^\dagger\phi_3)^2 \\
 & + \lambda_{12}(\phi_1^\dagger\phi_1)(\phi_2^\dagger\phi_2) + \lambda_{23}(\phi_2^\dagger\phi_2)(\phi_3^\dagger\phi_3) + \lambda_{31}(\phi_3^\dagger\phi_3)(\phi_1^\dagger\phi_1) \\
 & + \lambda'_{12}(\phi_1^\dagger\phi_2)(\phi_2^\dagger\phi_1) + \lambda'_{23}(\phi_2^\dagger\phi_3)(\phi_3^\dagger\phi_2) + \lambda'_{31}(\phi_3^\dagger\phi_1)(\phi_1^\dagger\phi_3), \\
 & -\mu_{12}^2(\phi_1^\dagger\phi_2) + \lambda_1(\phi_1^\dagger\phi_2)^2 + \lambda_2(\phi_2^\dagger\phi_3)^2 + \lambda_3(\phi_3^\dagger\phi_1)^2 + h.c.
 \end{aligned}$$

where CPV is introduced explicitly through complex parameters of the potential.

¹Note that adding extra Z_2 -respecting terms such as $(\phi_3^\dagger\phi_1)(\phi_2^\dagger\phi_3)$, $(\phi_1^\dagger\phi_2)(\phi_3^\dagger\phi_3)$, $(\phi_1^\dagger\phi_2)(\phi_1^\dagger\phi_1)$ and/or $(\phi_1^\dagger\phi_2)(\phi_2^\dagger\phi_2)$ does not change the phenomenology of the model. The coefficients of these terms, therefore, have been set to zero for simplicity.

The doublets are defined as

$$\phi_1 = \begin{pmatrix} H_1^+ \\ \frac{H_1^0 + iA_1^0}{\sqrt{2}} \end{pmatrix}, \quad \phi_2 = \begin{pmatrix} H_2^+ \\ \frac{H_2^0 + iA_2^0}{\sqrt{2}} \end{pmatrix}, \quad \phi_3 = \begin{pmatrix} G^+ \\ \frac{v+h+iG^0}{\sqrt{2}} \end{pmatrix}, \quad (3.1)$$

where ϕ_1 and ϕ_2 are the two *inert* doublets (odd under the Z_2) and ϕ_3 is the one *active* doublet (even under the Z_2) which plays the role of the SM-Higgs doublet. The symmetry of the potential is therefore respected by the vacuum alignment.

To make sure that the entire Lagrangian is Z_2 symmetric, we assign an even Z_2 parity to all SM particles, identical to the Z_2 parity of the only doublet that couples to them, i.e., the active doublet ϕ_3 [20]. With this parity assignment FCNCs are avoided as the extra doublets are forbidden to couple to fermions by Z_2 conservation.

We take S_1 to be the lightest neutral field from the inert doublets which now have a mixed CP-charge:

$$\begin{aligned} S_1 &= \frac{\alpha H_1^0 + \alpha H_2^0 - A_1^0 + A_2^0}{\sqrt{2\alpha^2 + 2}}, & S_2 &= \frac{-H_1^0 - H_2^0 - \alpha A_1^0 + \alpha A_2^0}{\sqrt{2\alpha^2 + 2}}, \\ S_3 &= \frac{\beta H_1^0 - \beta H_2^0 + A_1^0 + A_2^0}{\sqrt{2\beta^2 + 2}}, & S_4 &= \frac{-H_1^0 + H_2^0 + \beta A_1^0 + \beta A_2^0}{\sqrt{2\beta^2 + 2}}, \end{aligned} \quad (3.2)$$

and hence the DM candidate where α and β are the rotation angles [21]. Here, we study a simplified version of the I(2+1)HDM by imposing the following equalities $\mu_1^2 = \mu_2^2, \lambda_3 = \lambda_2, \lambda_{31} = \lambda_{23}, \lambda'_{31} = \lambda'_{23}$ which is sometimes referred to as the “dark democracy” limit. By imposing the “dark democracy” limit, the only two parameters that remain complex are μ_{12}^2 and λ_2 with θ_{12} and θ_2 as their CPV phases, respectively. Note that the *inert* sector is protected by a conserved Z_2 symmetry from coupling to the SM particles, therefore, the amount of CPV introduced here is not constrained by SM data, unlike what was presented in section 2.

3.2 Constraints on parameters

We take into account constraints that the boundedness of the potential, positive-definiteness of the Hessian and S, T, U parameters put on the model. Properties of all inert scalars are constrained by various experimental results. We have considered bounds from relic density observations, Gamma-ray searches, DM direct and indirect detection, the contribution of the new scalars to the W and Z gauge boson widths, null searches for charged scalars, invisible Higgs decays, Higgs total decay width and the $h \rightarrow \gamma\gamma$ signal strength.

3.3 Dark Matter relic density

Taking all (co)annihilation processes into account, we present three benchmark scenarios, A, B and C, in the low ($m_{S_1} < m_h/2$) and medium mass region ($m_h/2 < m_{S_1} < m_Z$): Scenario A where $m_{S_1} \ll m_{S_2}, m_{S_3}, m_{S_4}, m_{S_1^\pm}, m_{S_2^\pm}$, scenario B where $m_{S_1} \sim m_{S_3} \ll m_{S_2}, m_{S_4}, m_{S_1^\pm}, m_{S_2^\pm}$, and scenario C where $m_{S_1} \sim m_{S_3} \sim m_{S_2} \sim m_{S_4} \ll m_{S_1^\pm}, m_{S_2^\pm}$. For the numerical details of these benchmarks scenarios see [21].

In the CP-conserving version of the I(2+1)HDM (within the “dark democracy” limit) [22, 23], the inert scalar-gauge couplings are fixed, and given by the rotation angles $\theta_a = \theta_h = \pi/4$. They do

not depend on the mass splittings or the value of m_{S_1} . In the CPV case, however, these couplings depend on the rotation angles α and β in Eq. (3.2), which in turn depend on m_{S_i} . Higgs-inert scalar couplings are also modified with respect to the CP-conserving case which leads to different DM and LHC phenomenology of the model.

In Fig. 3, we show values of DM mass and Higgs-DM coupling that lead to the correct DM relic density for benchmarks A, B and C. Benchmark A with no coannihilation channels presents the standard behaviour of an $SU(2)$ DM candidate. In benchmark B for large values of $g_{S_1 S_1 h}$ the dominant annihilation channel is $S_1 S_1 \rightarrow \bar{b}b$ and, as there are also coannihilation channels, the relic density is usually too small. For smaller couplings the dominant channel is $S_1 S_3 \rightarrow Z \rightarrow q\bar{q}$ where the relevant cross section is too large. As the mass grows, the coannihilation channel gets weaker, allowing DM to obtain the proper relic density. For masses closer to $m_h/2$ the resonance annihilation dominates, following the same pattern as in benchmark A. In benchmark C, for small values of $g_{S_1 S_1 h}$ the dominant coannihilation channel is $S_1 S_4 \rightarrow Z \rightarrow f\bar{f}$ (light quarks), with a small contribution from $S_2 S_3 \rightarrow Z \rightarrow f\bar{f}$. For larger couplings the process $S_1 S_1 \rightarrow h \rightarrow b\bar{b}$ strongly increases the annihilation cross section.

In all scenarios, when DM mass is close to $m_h/2$ the Higgs-resonance annihilation takes over and only very small Higgs-DM couplings lead to the correct relic density value.

In the medium DM mass, $m_h/2 < m_{S_1} < m_{W^\pm, Z}$ the crucial channel for all benchmarks is the quartic process $S_1 S_1 \rightarrow W^+ W^-$ which does not depend on the rotation angles α and β . For this reason, all studied benchmarks as well as the CP-conserving scenarios follow a similar behaviour. For larger values of DM mass this annihilation is stronger, and cancellation with $S_1 S_1 \rightarrow h \rightarrow W^+ W^-$ is needed to get the proper relic density value. Therefore, the plot moves towards negative values of Higgs-DM coupling. In benchmarks B and C, other channels, such as $S_1 S_4 \rightarrow q\bar{q}$ or $S_3 S_3 \rightarrow W^+ W^-$ have a small contributions, leading to small deviations from the behaviour of benchmark A.

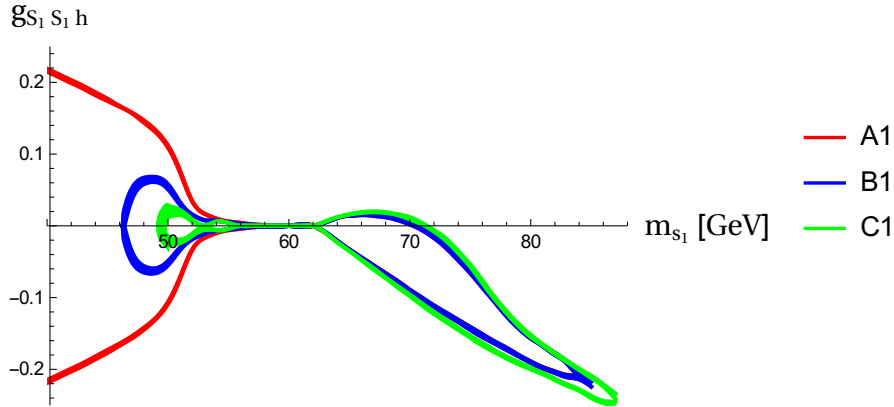


Figure 3: Relic density for low DM mass region in Scenarios A, B and C.

In Fig. 3, we have presented results for three sets of parameters in scenarios A, B, and C. It is clear that by changing the input set we can reach different regions of parameters space. Compare, for example, scenarios A and B, which differ only by the chosen values of θ_2 and θ_{12} . The performed scan shows that by varying the mass splitting and phases θ_2 and θ_{12} we can actually fill the empty regions inside the plots in Fig. 3. In Fig. 4 results obtained for various additional

sets of parameters are presented. We can fill the plot by different B and C scenarios, where the contribution from the coannihilation channels is crucial.

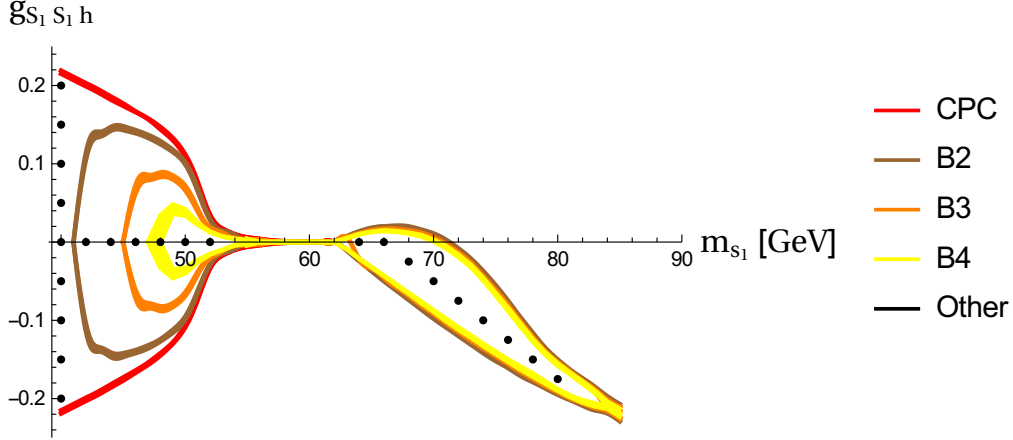


Figure 4: The relic density plots for different B and C scenarios where by changing the angles θ_2 and θ_{12} the whole region not accessible by the CP-conserving limit could be realised in the CPV case.

This is where the effect of CPV is evident. Direct and indirect detection experiments as well as LHC limits constrain the Higgs-DM coupling severely in all Higgs-portal DM type models. However, in the CPV I(2+1)HDM, owing to the freedom in the strength of inert-gauge couplings, one can opt for very small Higgs-DM couplings while getting the proper relic density and surviving all DM detection and LHC experiments.

4. Conclusion

We have looked into scalar extensions of the SM with CPV. We have presented LHC signatures of a Type-I 2HDM with CPV. In such a model with two active doublets contributing to the EWSB, the amount of CPV is very constrained. Moreover, such a model does not provide a DM candidate. We further extend the scalar sector to a 3HDM with two inert and one active doublet. The active doublet plays the role of the SM-Higgs doublet. The extended inert sector accommodates DM and an unbounded amount of CPV. We have studied DM phenomenology of such a model.

Acknowledgements The author's research is financially supported by the Academy of Finland project "The Higgs Boson and the Cosmos" and project 267842. She also acknowledges the H2020-MSCA-RICE-2014 grant no. 645722 (NonMinimalHiggs).

References

- [1] ATLAS Collaboration, *Phys.Lett.* **B716** (2012) 1.
- [2] CMS Collaboration, *Phys.Lett.* **B716** (2012) 30.
- [3] G. Jungman, M. Kamionkowski and K. Griest, *Phys.Rept.* **267** (1996) 195.

- [4] G. Bertone, D. Hooper and J. Silk, *Phys.Rept.* **405** (2005) 279.
- [5] L. Bergstrom, *Rept.Prog.Phys.* **63** (2000) 793.
- [6] P. A. R. Ade *et al.* [Planck Collaboration], arXiv:1502.01589 [astro-ph.CO].
- [7] S. Dimopoulos and L. Susskind, *Phys. Lett. B* **81**, 416 (1979)
- [8] J. M. Cline, hep-ph/0609145.
- [9] N. G. Deshpande and E. Ma, *Phys.Rev.* **D18** (1978) 2574.
- [10] E. Ma, *Phys.Rev.* **D73** (2006) 077301,
- [11] R. Barbieri, L. J. Hall and V. S. Rychkov, *Phys. Rev.* **D74** (2006) 015007.
- [12] L. Lopez Honorez, E. Nezri, J. F. Oliver and M. H. G. Tytgat, *JCAP* **0702** (2007) 028.
- [13] V. D. Barger, J. L. Hewett and R. J. N. Phillips, *Phys. Rev. D* **41** (1990) 3421; Y. Grossman, *Nucl. Phys. B* **426** (1994) 355; A. G. Akeroyd, *Phys. Lett. B* **377** (1996) 95.
- [14] M. Aoki, S. Kanemura, K. Tsumura and K. Yagyu, *Phys. Rev. D* **80** (2009) 015017.
- [15] S. Davidson and H. E. Haber, *Phys. Rev. D* **72**, 035004 (2005) [*Phys. Rev. D* **72**, 099902 (2005)].
- [16] V. Keus, S. F. King, S. Moretti and K. Yagyu, *JHEP* **1604**, 048 (2016) [arXiv:1510.04028 [hep-ph]].
- [17] M. E. Peskin and T. Takeuchi, *Phys. Rev. Lett.* **65**, 964 (1990); *Phys. Rev. D* **46**, 381 (1992).
- [18] W. Grimus, L. Lavoura, O. M. Ogreid and P. Osland, *Nucl. Phys. B* **801**, 81 (2008);
H. E. Haber and D. O’Neil, *Phys. Rev. D* **83**, 055017 (2011).
- [19] I. P. Ivanov, V. Keus and E. Vdovin, *J. Phys. A* **45**, 215201 (2012) [arXiv:1112.1660 [math-ph]].
- [20] I. P. Ivanov and V. Keus, *Phys. Rev. D* **86**, 016004 (2012) [arXiv:1203.3426 [hep-ph]].
- [21] A. Cordero-Cid, J. Hernández-Sánchez, V. Keus, S. F. King, S. Moretti, D. Rojas and D. Sokolowska, *JHEP* **1612**, 014 (2016) [arXiv:1608.01673 [hep-ph]].
- [22] V. Keus, S. F. King, S. Moretti and D. Sokolowska, *JHEP* **1411** (2014) 016.
- [23] V. Keus, S. F. King, S. Moretti and D. Sokolowska, *JHEP* **1511**, 003 (2015) [arXiv:1507.08433 [hep-ph]].